

Dissecting an Allosteric Switch in Caspase-7 Using Chemical and Mutational Probes*

Received for publication, April 7, 2009, and in revised form, June 3, 2009. Published, JBC Papers in Press, July 6, 2009, DOI 10.1074/jbc.M109.001826

Jeanne A. Hardy¹ and James A. Wells²

From Sunesis Pharmaceuticals, South San Francisco, California 94080

Apoptotic caspases, such as caspase-7, are stored as inactive protease zymogens, and when activated, lead to a fate-determining switch to induce cell death. We previously discovered small molecule thiol-containing inhibitors that when tethered revealed an allosteric site and trapped a conformation similar to the zymogen form of the enzyme. We noted three structural transitions that the compounds induced: (i) breaking of an interaction between Tyr-223 and Arg-187 in the allosteric site, which prevents proper ordering of the catalytic cysteine; (ii) pinning the L2' loop over the allosteric site, which blocks critical interactions for proper ordering of the substrate-binding groove; and (iii) a hinge-like rotation at Gly-188 positioned after the catalytic Cys-186 and Arg-187. Here we report a systematic mutational analysis of these regions to dissect their functional importance to mediate the allosteric transition induced by these compounds. Mutating the hinge Gly-188 to the restrictive proline causes a massive ~6000-fold reduction in catalytic efficiency. Mutations in the Arg-187–Tyr-223 couple have a far less dramatic effect (3–20-fold reductions). Interestingly, although the allosteric couple mutants still allow binding and allosteric inhibition, they partially relieve the mutual exclusivity of binding between inhibitors at the active and allosteric sites. These data highlight a small set of residues critical for mediating the transition from active to inactive zymogen-like states.

Caspases are a family of dimeric cysteine proteases whose members control the ultimate steps for apoptosis (programmed cell death) or innate inflammation among others (for reviews, see Refs. 1 and 2). During apoptosis, the upstream initiator caspases (caspase-8 and -9) activate the downstream executioner caspases (caspase-3, -6, and -7) via zymogen maturation (3). The activated executioner caspases then cleave upwards of 500 key proteins (4–6) and DNA, leading to cell death. Due to their pivotal role in apoptosis, the caspases are involved both in embryonic development and in dysfunction in diseases including cancer and stroke (7). The 11 human caspases share a common active site cysteine-histidine dyad (8), and derive their name, cysteine aspartate proteases, from their exquisite specificity for cleaving substrate proteins after spe-

cific aspartate residues (9–13). Thus, it has been difficult to develop active site-directed inhibitors with significant specificity for one caspase over the others (14). Despite difficulties in obtaining specificity, there has been a long-standing correlation between efficacy of caspase inhibitors *in vitro* and their ability to inhibit caspases and apoptosis *in vivo* (for review, see Ref. 31). Thus, a clear understanding of *in vitro* inhibitor function is central to the ability control caspase function *in vivo*.

Caspase-7 has been a paradigm for understanding the structure and dynamics of the executioner caspases (15–21). The substrate-binding site is composed of four loops; L2, L3, and L4 are contributed from one-half of the caspase dimer, and L2' is contributed from the other half of the caspase dimer (Fig. 1). These loops appear highly dynamic as they are only observed in x-ray structures when bound to substrate or substrate analogs in the catalytically competent conformation (17–19, 22) (Fig. 1B).

A potential alternative to active site inhibitors are allosteric inhibitors that have been seeded by the discovery of selective cysteine-tethered allosteric inhibitors for either apoptotic executioner caspase-3 or apoptotic executioner caspase-7 (23) as well as the inflammatory caspase-1 (24). These thiol-containing compounds bind to a putative allosteric site through disulfide bond formation with a thiol in the cavity at the dimer interface (Fig. 1A) (23, 24). X-ray structures of caspase-7 bound to allosteric inhibitors FICA³ and DICA (Fig. 2) show that these compounds trigger conformational rearrangements that stabilize the inactive zymogen-like conformation over the substrate-bound, active conformation. The ability of small molecules to hold mature caspase-7 in a conformation that mimics the naturally occurring, inactive zymogen state underscores the utility and biological relevance of the allosteric mechanism of inhibition. Several structural changes are evident between these allosterically inhibited and active states. (i) The allosteric inhibitors directly disrupt an interaction between Arg-187 (next to the catalytic Cys-186) and Tyr-223 that springs the Arg-187 into the active site (Fig. 3), (ii) this conformational change appears to be facilitated by a hinge-like movement about Gly-188, and (iii) the L2' loop folds down to cover the allosteric inhibitor and assumes a zymogen-like conformation (Fig. 1C) (23).

Here, using mutational analysis and small molecule inhibitors, we assess the importance of these three structural units to

* This work was supported, in whole or in part, by National Institutes of Health Grant Postdoctoral Fellowship GM65048 (to J. H.).

¹ Present address: Dept. of Chemistry, University of Massachusetts, Amherst, MA.

² To whom correspondence should be addressed: Depts. of Pharmaceutical Chemistry and Molecular and Cellular Pharmacology, UCSF-Box 2552, San Francisco, CA 94143-2552. Tel.: 415-514-4498; Fax: 415-514-4507; E-mail: jim.wells@ucsf.edu.

³ The abbreviations used are: FICA, 5-fluoro-1H-indole-2-carboxylic acid (2-mercapto-ethyl)-amide; DICA, 2-(2,4-dichlorophenoxy)-N-(2-mercapto-ethyl)-acetamide; z-DEVD-fmk, Cbz-Asp-Glu-Val-Asp-fluoromethyl ketone; Ac-DEVD-AFC, acetyl-Asp-Glu-Val-Asp-aminofluorocoumarin; CHAPS, 3-[(3-cholamidopropyl)dimethylammonio]-1-propanesulfonate.

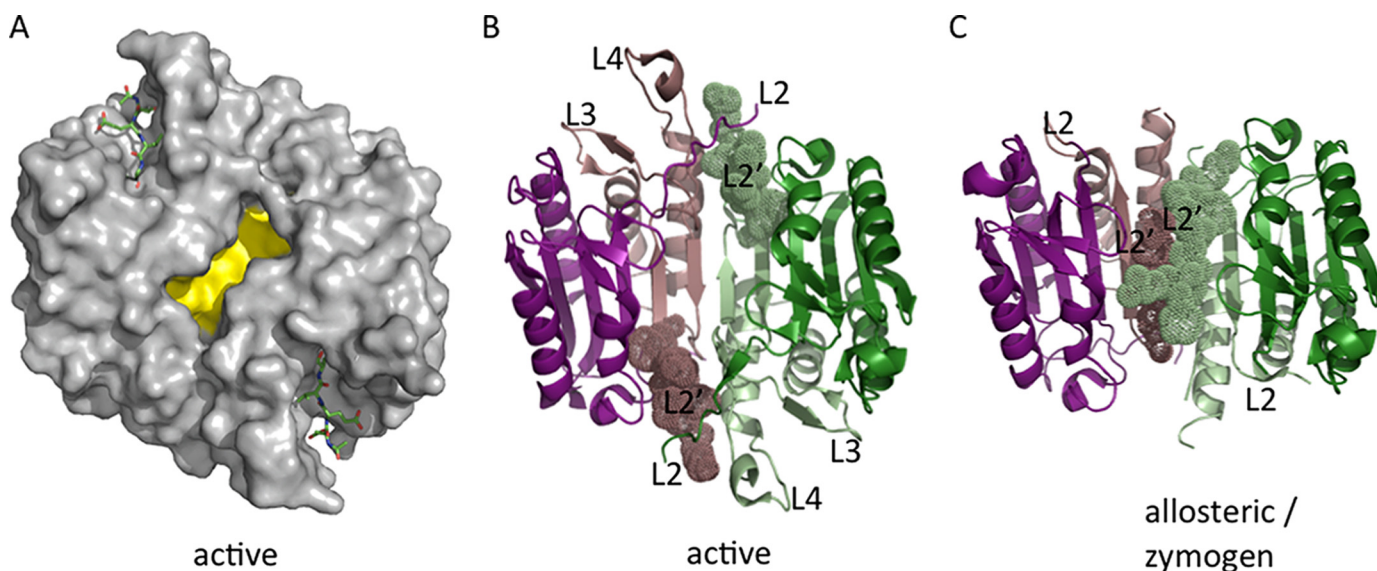


FIGURE 1. Allosteric site and dimeric structure in caspase-7. A, the surface of active site-bound caspase-7 shows a large open allosteric (yellow) site at the dimer interface. This cavity is distinct from the active sites, which are bound with the active site inhibitor DEVD (green sticks). B, large subunits of caspase-7 dimers (dark green and dark purple) contain the active site cysteine-histidine dyad. The small subunits (light green and light purple) contain the allosteric site cysteine 290. The conformation of the substrate-binding loops (L2, L2', L3, and L4) in active caspase-7 (Protein Data Bank (PDB) number 1f1j) is depicted. The L2' loop (spheres) from one-half of the dimer interacts with the L2 loop from the other half of the dimer. C, binding of allosteric inhibitors influences the conformation of the L2' loop (spheres), which folds over the allosteric cavity (PDB number 1shj). Subunit rendering is as in panel A. Panels A, B, and C are in the same orientation.

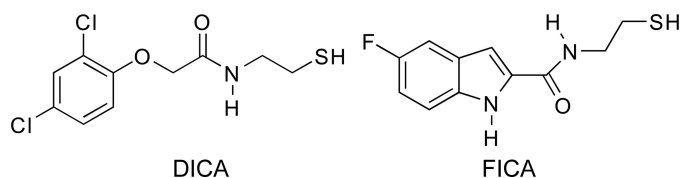


FIGURE 2. Structure of allosteric inhibitors DICA and FICA. DICA and FICA are hydrophobic small molecules that bind to an allosteric site at the dimer interface of caspase-7. Binding of DICA/FICA is mediated by a disulfide between the compound thiol and Cys-290 in caspase-7.

modulate both the inhibition of the enzyme and the coupling between allosteric and active site labeling. Our data suggest that the hinge movement and pinning of the L2-L2' are most critical for transitioning between the active and inactive forms of the enzyme.

EXPERIMENTAL PROCEDURES

Constructs and Protein Purification—The caspase-7 large subunit expression plasmid pJH08 was created by subcloning the PCR product encoding residues 57–198 from a pro-caspase-7 expression plasmid (a gift from Dr. Guy Salvesen, Burnham Institute) into pRSET (amp^r, Invitrogen). The small subunit coding sequence for caspase-7 residues 210–303 plus the amino acids QLH₆ was introduced into pBB75 (kan^r, a gift of Prof. Yigong Shi, Tsinghua University) to generate pJH07 encoding a C-terminal His₆ tag following the small subunit coding sequence. All of the individual point mutations were introduced by oligonucleotide-directed mutagenesis into pJH07 or pJH08. The resulting plasmids were cloned and sequenced to confirm the presence of the mutation and absence of the wild-type sequence. To produce the mutant caspase-7 described here, the appropriate large subunit- or small subunit-expressing plasmids were transformed simultaneously into *Escherichia coli* strain BL21(DE3). Protein expression was induced with 100

μg/ml isopropyl β-D-1-thiogalactopyranoside and allowed to proceed for 12–18 h at 14 °C. Each caspase variant was purified by affinity chromatography on a nickel-nitrilotriacetic acid superflow column (Qiagen) developed with a step gradient of 250 mM imidazole. Mutants were further purified using ion exchange chromatography on a 5-ml High-Q column (Bio-Rad) with a linear gradient from 50 to 750 mM NaCl. The purity of all mutants was assessed by SDS-PAGE gel stained with Coomassie Blue (Bio-Rad) and found to be >95% pure. The concentration of active sites was determined by active site titration with an irreversible active site inhibitor z-DEVD-fmk (Cbz-Asp-Glu-Val-Asp-fluoromethyl ketone, Calbiochem). Inactivation as a result of active site titration was observed by monitoring remaining caspase activity in the fluorescence assay described below.

Caspase Modification—Time, reductant, and compound concentrations were co-varied within the ranges listed to induce various levels of thiol modification. Caspase-7 mutants (4 μM) were incubated in Tris-EDTA buffer for 1–3 h with 0.1–5 mM β-mercaptoethanol, 0.05–0.25 mM FICA or DICA, or 0.01–0.04 mM z-DEVD-fmk (Calbiochem). To observe mutual exclusivity, after the first modification, the second compound was added and incubated an additional hour. Modification of both small and large subunits was measured using a QSTAR Pulsar-i, quadrupole time-of-flight mass spectrometer (Applied Biosystems/MDS Sciex). We assume uniform ionization of the modified and unmodified caspase and routinely observe S.D. = ±2% for modification.

Activity Assays—Modified or unmodified caspase-7 wild type or variant (final concentration ranges of 160–400 nM) was added to reaction buffer (10% polyethylene glycol 400, 5 mM CaCl₂, 100 mM HEPES, pH 7.0, 0.1% CHAPS, and 5 mM β-mercaptoethanol). The addition of 5 μM fluorogenic substrate, Ac-

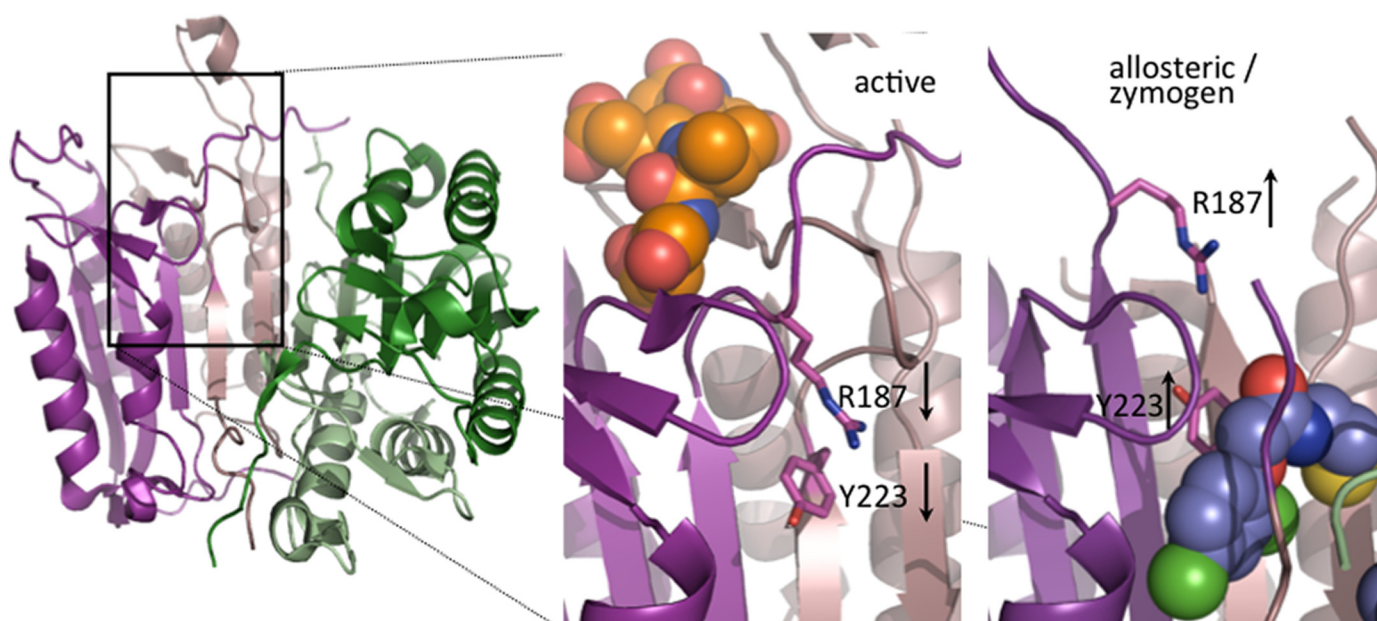


FIGURE 3. **Movement of L2' blocking arm.** The region of caspase-7 encompassing the allosteric couple Arg-187 and Tyr-223 is boxed. The inset shows the down orientation of Arg-187 and Tyr-223 in the active conformation with DEVD substrate mimic (orange spheres) in the active site. In the allosteric/zymogen conformation, Arg-187 and Tyr-223 are pushed up by DICA (blue spheres).

DEVD-AFC (acetyl-Asp-Glu-Val-Asp-aminofluorocoumarin, Alexis Biochemicals), initiated the reaction. Assays were performed on a microplate spectrofluorometer GeminiXS (Molecular Devices) with an excitation wavelength of 365 nm and an emission wavelength of 495 nm. For wild type and most caspase-7 variants, kinetic data were collected over a 7-min assay run at room temperature. For the G188P and G188L mutations,⁴ kinetic data were collected over an 8-h period. To determine the K_m and k_{cat} values, activity was measured as a function of substrate concentration over a range from 0 to 0.8 mM. Data from this analysis were fitted to a rectangular hyperbolic curve in Prism Software (GraphPad). Data from three or more independent experiments were averaged.

For G188P and G188L, K_m is not significantly altered from wild type, but the turnover (k_{cat}) is dramatically reduced. Although surface mutations such as these do not typically cause gross misfolding, there are three lines of biochemical evidence to suggest that this residual activity is not due to wild-type contamination or gross misfolding of the mutants. First, each mutant was tested three times from two different preparations and gave consistent results and protein yields (Table 1). Second, the final chromatographic step gave predominantly a single symmetrical peak that eluted where the wild-type enzyme does (data not shown). SDS-PAGE showed the mutant proteins to be on average >95% pure. We also do not see evidence of wild-type contamination as assessed by mass spectrometry whose detection limit is close to 1%. Lastly, the G188P mutant is specifically and quantitatively labeled with each of the allosteric inhibitors at the thiol at the dimer interface although there are four other thiols in the enzyme (Table 2). We would not expect any of these to be the case were the protein preparations grossly misfolded or contaminated with wild-type protein.

⁴ Mutant nomenclature lists the wild-type amino acid in single letter code and its position followed by the mutant residue.

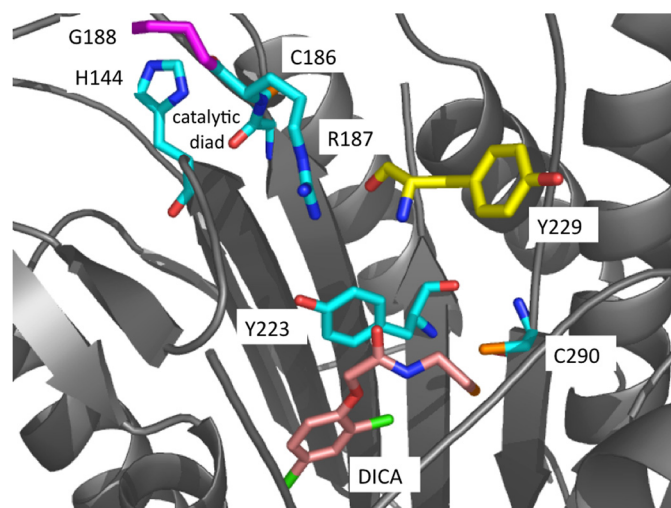


FIGURE 4. **Rational design of mutations in the caspase-7 allosteric couple.** Interrogated residues are shown in stick representation to clarify the steric relationship between these residues. Allosteric couple residues Arg-187 and Tyr-223 and catalytic dyad residues His-144 and Cys-186 are drawn in cyan sticks. Allosteric inhibitor DICA is in orange sticks, and the cysteine residue to which it covalently binds (Cys-290) is marked. Residue Gly-188 is in purple sticks, and Tyr-229 is in yellow sticks. This figure is based on the allosterically inhibited complex of caspase-7 with DICA (PDB number 1shj).

RESULTS

Design and Characterization of Mutations That Couple Active and Allosterically Inhibited Conformers of Caspase-7—

We generated a panel of mutants to test the functional impact of rotating about the Gly-188 hinge, breaking the interaction between the allosteric couple Arg-187–Tyr-223, or packing of the L2' loop (Fig. 4). These were expressed in *E. coli*, purified to >95% homogeneity, and kinetic parameters were determined by standard Michaelis-Menten analysis (Table 1). The G188P mutation, which should introduce a severe restriction in the rotation about Gly-188, caused a dramatic ~6000-fold reduc-

TABLE 1

Catalytic properties of caspase-7 variants

Data are from duplicate experiments performed on three separate days. WT, wild type.

Mutant	K_m	k_{cat}	$10^6 \times k_{cat}/K_m$	Effect on k_{cat}/K_m (fraction of WT activity)
	μM	s^{-1}	$M^{-1} s^{-1}$	
WT	10 ± 4	0.51 ± 0.01	0.051	1.00
R187A	36 ± 5	0.49 ± 0.06	0.014	0.27
R187M	22 ± 9	0.78 ± 0.47	0.035	0.69
R187N	58 ± 9	0.20 ± 0.10	0.003	0.06
R187G	43 ± 4	0.37 ± 0.04	0.009	0.18
R187W	80 ± 3	0.13 ± 0.05	0.0002	3.9×10^{-3}
R187K	89 ± 27	0.27 ± 0.13	0.003	0.06
G188P	13 ± 8	$(1 \pm 0.15) \times 10^{-4}$	7.6×10^{-6}	1.5×10^{-5}
G188L	14 ± 2	0.02 ± 0.01	0.0011	0.02
Y223A	123 ± 16	0.38 ± 0.16	0.003	0.06
Y223F	12 ± 5	0.44 ± 0.33	0.036	0.71
Y223W	10 ± 2	0.33 ± 0.11	0.033	0.65
Y223E	14 ± 1	0.28 ± 0.04	0.020	0.39
Y223D	9 ± 2	0.56 ± 0.14	0.062	1.22
Y229W	163 ± 14	0.02 ± 0.001	0.0001	1.9×10^{-3}
C290T	43 ± 25	0.63 ± 0.22	0.014	0.27
C290N	13 ± 4	0.53 ± 0.01	0.040	0.78

tion in catalytic efficiency (k_{cat}/K_m). The less restrictive G188L mutation caused much more modest 46-fold reduction in catalytic efficiency. Virtually all the reduction in catalytic efficiency for both mutations is manifested in k_{cat} . For amide bond hydrolysis, acylation is rate-limiting, and therefore K_m is a reasonable measure of the substrate dissociation constant (25–27). These data would suggest that although the substrate can bind the same way, the hinge movement at Gly-188 is critical for the positioning of the catalytic Cys-186.

Sandwiched between the Gly-188 hinge and the catalytic Cys-186 is Arg-187. The Arg-187 is involved in the allosteric couple with Tyr-223, which gets broken by tethering the allosteric inhibitors (Fig. 3). A series of side-chain truncation mutants (R187M, R187A, and R187G) caused only 2–5-fold reductions in catalytic efficiency. This suggests that the guanido functionality or alkyl side-chain does not participate to a large degree in stabilizing the active conformation. Neutralizing the charge and repositioning the hydrogen-bonding functionality in the R187N mutant or imposing a larger hydrophobic side-chain in the R187W mutant caused larger 17-fold reductions. The effects of all these mutants appeared both in k_{cat} and in K_m , suggesting that substrate binding and catalytic group positioning were affected somewhat. Mutations at Tyr-223 were even less impactful. The side-chain truncation series (Y223A, Y223F) had minimal impact, as did the larger hydrophobic mutant Y223W or the acidic mutants Y223D and Y223E.

The L2 loop folds beneath Tyr-229 and L2' folds above Tyr-229 in the active conformer (Fig. 4). When the larger tryptophan was introduced, the Y229W mutant caused a 50-fold reduction in catalytic efficiency. Virtually all of this was the result of an increased K_m , consistent with the L2' loop being critical for substrate binding. Two other mutants were produced, C290T and C290N, which mutated the residue to which the allosteric thiol inhibitors tether. These had virtually no impact on catalysis, suggesting that the inhibition caused by the allosteric tethered compounds was not due to simply masking this residue.

TABLE 2

Ability of DICA/FICA to bind and inhibit caspase-7 mutants

All mutants were assayed uniformly under conditions that allowed full conjugation of DICA to wild-type caspase-7. Thus the assay was not optimized to find conditions that allowed full occupation of both the allosteric and active sites for each of the mutants. WT, wild type. ND, not determined.

Mutation	Fractional DICA conjugation	Fractional FICA conjugation	FICA/DICA inhibition
WT	100	75	Yes
R187A	100	94	Yes
R187M	100	84	Yes
R187N	100	100	Yes
R187G	100	86	Yes
R187W	100	81	Yes
R187K	100	100	Yes
G188P	100	100	ND
Y223A	100	100	Yes
Y223F	100	91	Yes
Y223W	100	62	Yes
Y223E	84	53	Yes
Y223D	42	42	Yes
Y229W	100	100	Yes
C290N	0	0	No
C290T	0	0	No

In sum, mutations at the allosteric couple suggest that this interaction is not so critical for stabilizing the active conformer of caspase-7. In contrast, swiveling about the Gly-188 is critical for proper positioning of the catalytic cysteine, and binding of the L2' loop against Tyr-229 is important for substrate binding.

As with any mutational analysis, it is possible that these effects were caused by misfolding of the protein. However, two lines of evidence would suggest that misfolding is not a systematic problem. First, most of the mutations (including those at Gly-188) had only small effects on K_m , suggesting that substrate can bind. Also, what subtle changes were observed in K_m are statistically significant from wild type, which suggests that the activity observed is not from a small fraction of wild-type-like enzyme but rather a bulk of slightly altered enzyme. Secondly, the enzymes were expressed and purified at wild-type levels, suggesting that the mutations did not introduce severely destabilizing changes to the protein typical of aberrant folding variants.

Effect of Mutation in Allosteric Couple on Allosteric Labeling and Inhibition—We next probed the effect that mutations in the Arg-187–Tyr-223 couple have on three parameters: (i) the ability of the allosteric compounds FICA and DICA to tether, (ii) their ability to inhibit the enzyme, and (iii) their ability to prevent labeling of the catalytic cysteine with the active site titrant. Previously, we found that the strength of the interaction of allosteric inhibitors FICA and DICA is related to the rate at which FICA and DICA bind to caspase-7 and that the amount of FICA or DICA binding is linearly related to the level of inhibition (23). DICA binds to wild-type caspase-7 more rapidly and more tightly than FICA (as determined by reductant titration, data not shown). Wild-type and caspase-7 mutants were incubated for a fixed period of time (2 h) followed by mass spectrometry to determine the extent of binding of FICA or DICA (Table 2). All of the mutants were able to bind DICA as well as or better than wild type except for Y223D, Y223E, C290N, and C290T. The diminished binding to Y223D and Y223E is possibly due to an unfavorable interaction between the negative charge and the very hydrophobic DICA molecules. C290D and C290N are incapable of disulfide bonding with

DICA or FICA. We also see reduced tethering of DICA to the G188L mutant yet no reduction in tethering to the G188P mutant. Modeling in the DICA wild-type structure suggests that this difference is from the larger leucine side-chain impinging binding of the DICA.

The level of FICA binding was lower than the level of DICA binding in several of the mutant proteins. Nevertheless, all of the mutants were capable of binding at some level. As binding of FICA and DICA depends on the time and reductant concentration, it is likely that all mutant proteins can be fully occupied by FICA and DICA under the appropriate conditions. The possible exceptions are Y223E and Y223D, in which a negative charge decreases affinity for neutral FICA and DICA. Importantly, all of the proteins with mutations of the allosteric couple retain the ability to be inhibited by FICA and DICA (Table 2). Moreover, the level of inhibition by FICA and DICA correlate with the extent of compound binding.

Effect of Mutations in the Allosteric Couple on Mutual Exclusivity—We next designed experiments to probe the role of the mutated residues in coupling the allosteric and active sites. In wild-type caspase-7, the active site binders like peptide inhibitor DEVD-fmk prevent binding of synthetic allosteric inhibitors DICA and FICA and vice versa (23). Thus, binding at the active site is mutually exclusive (competitive) with binding at the allosteric site, although the compounds do not physically touch. We reasoned that if the allosteric couple Arg-187–Tyr-223 was essential for enforcing the mutual exclusivity of the active and allosteric sites, then mutation of these residues might break the tight mutual exclusivity observed in wild-type caspase-7.

To probe the mutual exclusivity of mutants, we performed order of addition experiments with active and allosteric site inhibitors. We incubated caspase-7 mutants first with allosteric inhibitors DICA or FICA and then added active site-directed inhibitor DEVD-fmk (Fig. 5). Mutual exclusivity of wild-type caspase-7 is demonstrated by the fact that the sum total of binding of DEVD active site titrant to the large subunit plus either FICA or DICA tethering to the small subunit never exceeded 100%. For example, when DICA labeling of the wild-type allosteric site proceeded until 97% of the small subunits were bound, then only the remaining 3% of unlabeled large subunits bound to DEVD (Fig. 5A). When FICA labeling is allowed to proceed only until 75% of the small subunits are bound, only the remaining unlabeled 25% of large subunits can subsequently be bound (Fig. 5B). The C290N and C290T mutations displayed the tight 100% limit like the wild-type protein because these mutations obliterate the thiol required for disulfide formation with FICA and DICA. In the experiments reported here, as well as in similar experiments not shown, the tight mutual exclusivity between the active and allosteric sites in wild-type caspase-7 was always maintained (Fig. 5).

In contrast, all of the mutations at both Arg-187 and Tyr-223 break the mutual exclusivity (Fig. 5). Under the conditions tested, up to 180% binding was observed, which reflects the fact that both the active and the allosteric sites are nearly fully occupied with on average 1.8 compounds (active site inhibitor plus allosteric site inhibitor) bound per monomer. Replacement of Arg-187 by Ala, Met, Asn, Trp, or Gly allowed simultaneous

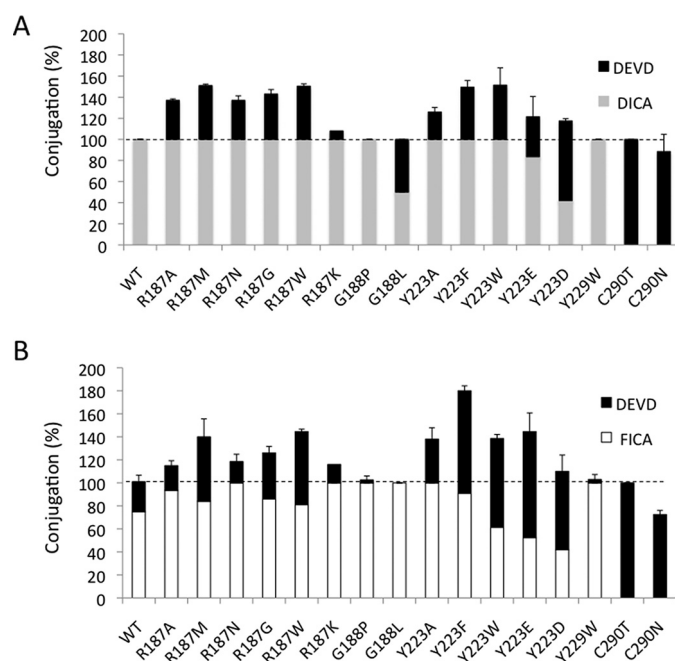


FIGURE 5. Monitoring mutual exclusivity of binding at the active and allosteric sites of caspase-7 variants. A, the proportion of caspase-7 small subunit bound by DICA and large subunits bound by DEVD are shown. Caspase-7 variants were first incubated with the allosteric inhibitor DICA (gray bars) and then incubated with active site inhibitor DEVD-fmk (black bars). Binding of DICA to Cys-290 in the small subunits and binding of DEVD to the active site cysteine in the large subunits was monitored by mass spectrometry. WT, wild type. B, as in A, but caspase-7 variants were first incubated the allosteric inhibitor FICA (white bars) and then with active site inhibitor DEVD-fmk (black bars).

occupation of the active and allosteric sites up to 140%. The most conservative of all the mutations, R187K that most closely mimics the Arg side chain, retained the highest degree of mutual exclusivity (<120% for both FICA and DICA).

In sharp contrast, when the order of binding was reversed such that caspase-7 mutants were first incubated with active site inhibitor DEVD-fmk and then incubated with the allosteric inhibitors DICA or FICA, we observed almost complete retention of the mutual exclusivity (Fig. 6). When caspase-7 mutants were first labeled with DEVD-fmk and then FICA, the total sum of stoichiometries did not exceed unity. When DICA was added in the second step, the greatest level of conjugation was 120% total. This is a substantial decrease relative to the reverse-ordered reaction where many mutants displayed binding in excess of 140%. The order of addition dependence suggests that locking loops into the active conformation in the first step lowers the ability to label with the allosteric site compounds FICA or DICA. The fact that the tight mutual exclusivity of the active and allosteric sites is broken in both Arg-187 and Tyr-223 mutants, but not in Trp-229 or Gly-188, mutants strongly suggests that Arg-187 and Tyr-223 alone are sufficient for enforcing the tight mutual exclusivity of wild-type caspase-7.

DISCUSSION

These data provide insights into the functional importance of three regions for modulating the conformational transition between the active form (on form) and allosterically inhibited form (off form) of caspase-7: the hinge, the allosteric couple,

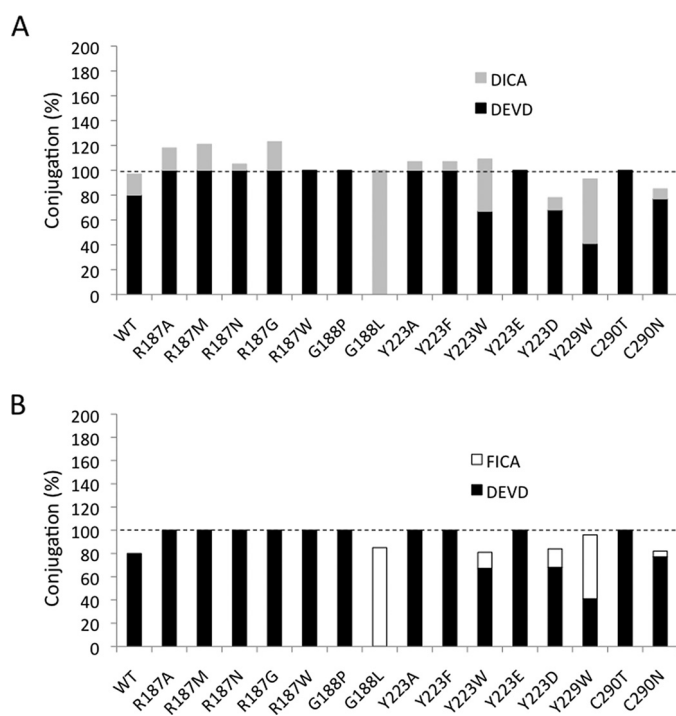


FIGURE 6. Effect of order of addition on mutual exclusivity of active and allosteric sites. A, caspase-7 variants were first incubated with active site inhibitor DEVD-fmk (black bars) and then with the allosteric inhibitor DICA (gray bars). Binding of DICA to Cys-290 in the small subunits and binding of DEVD to the active site cysteine in the large subunits was monitored by mass spectrometry. WT, wild type. B, as in A, but caspase-7 variants were first incubated with active site inhibitor DEVD-fmk (black bars) and then with the allosteric inhibitor FICA (white bars).

and the L2' loop. Previous structural studies have shown that the allosterically inhibited conformation is very close to the zymogen form of caspase-7 (8). The mutational analysis identifies Gly-188 as a critical hinge determinant for transitioning between the on and off forms. The G188P mutation causes an ~6000-fold reduction in catalytic efficiency and is about 200 times more impactful than the G188L mutation. Moreover, virtually all of these effects are on k_{cat} . These data suggest that rotation about the main-chain amide is critical for alignment of the catalytic apparatus when transitioning between the off and on forms of the enzyme.

Allosteric couples exist in both the executioner caspases (caspase-3 and -7) and the inflammatory caspase-1 (23, 24, 28). For caspase-7, the couple is the Arg-187–Tyr-223 dyad, whereas the structurally analogous pair in caspase-1 is the Arg-286–Glu-390 salt bridge. However, the magnitudes of the disruptive effects seen for mutating these couples are very different. Mutation of the Arg-187–Tyr-223 in caspase-7 shows rather modest effects, about 3–17-fold reductions in catalytic efficiency depending on the mutation couple. In contrast, mutation of the Arg-286–Glu-390 salt bridge in caspase-1 causes a nearly 300-fold reduction (24, 28). This difference may be a consequence of the more extensive 18-member hydrogen-bonded allosteric network in caspase-1 when compared with the four-member network in caspase-7.

The difference in functional impact for mutating the couples may also reflect the relative equilibrium distribution between on and off states for these enzymes in the absence of bound

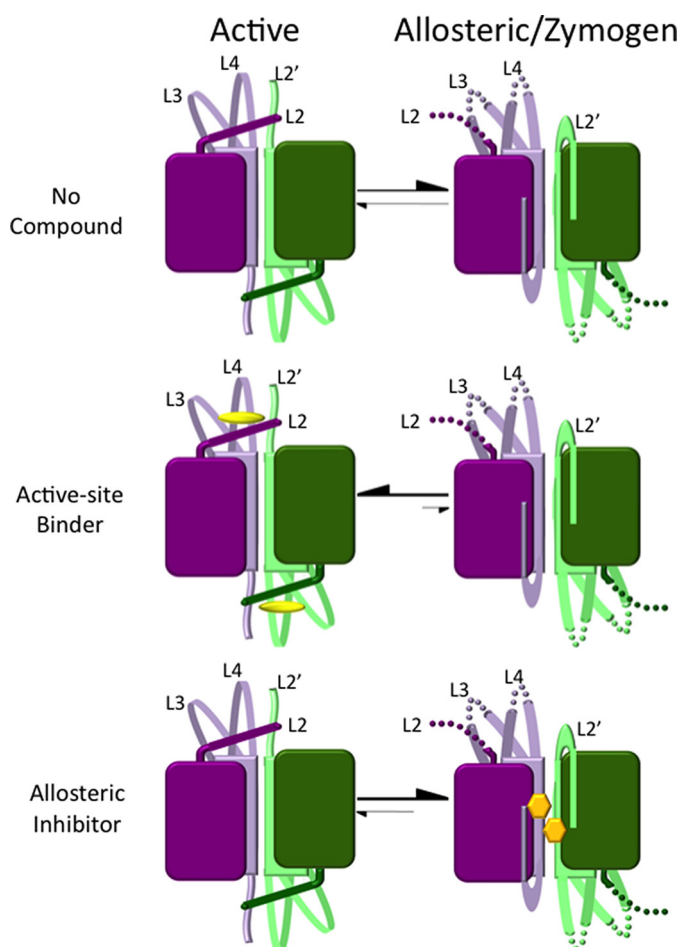


FIGURE 7. Model of conformational equilibrium of wild type and allosteric-couple mutations in caspase-7. The conformational equilibrium in the presence of an active site binder lies stringently toward the active conformation. The conformational equilibrium when bound to the allosteric inhibitor lies less stringently toward the allosteric/zymogen state, as indicated by the size of the arrows.

substrate, as shown in the model in Fig. 7. For example, recent conformationally selective antibodies that were separately raised to recognize caspase-1 which is locked into either the on or off state, show that the apo-enzyme favors binding to the off state antibody by a factor of at least 100:1 (29). Caspase-1 also shows pronounced positive cooperativity, suggesting that substrate binding drives it into the active conformation (24, 28). Moreover, the crystal structure of caspase-1 in the absence of an active site ligand shows it in an off state that is virtually identical to that of the allosterically inhibited caspase-1 (22, 30). In contrast, caspase-7 shows much weaker positive cooperativity, and the x-ray structure of apo-caspase-7 shows it in a partially active conformation with the L2 loop in the active conformation but the L2' loop and Arg-187 in a zymogen-like conformation. These data suggest that apo-caspase-7 favors the on state to a greater degree than caspase-1.

Mutating the Arg-187–Tyr-223 couple in caspase-7 breaks the mutual exclusivity of binding at the active and allosteric sites, which allows the sum of active site and allosteric site inhibitors to exceed unity (Fig. 5). This suggests that the allosteric couple links conformational changes from the allosteric and active site. Nonetheless, when the allosteric couple is

mutated, the allosteric tethered compounds can still inhibit enzyme activity. This suggests another interaction capable of enforcing allosteric inhibition, namely locking the L2' loop over the allosteric site by direct interactions with the allosteric inhibitors, FICA or DICA. This "closing" of the L2' loop is further supported by the order-of-addition experiment (Fig. 6) where the prior addition of the active site inhibitor DEVD-fmk prevents further labeling with allosteric inhibitors even for mutants that mutate the allosteric couple. This suggests that binding of the L2' loop over the allosteric site, which is facilitated by the positive interactions made between the L2' loop and FICA and DICA, is sufficient to inhibit caspase-7. Our data suggest that interactions between the L2' loop and compounds that occupy the allosteric site are important for allosteric inhibition.

The mutational experiments in caspase-7 and previously on caspase-1 suggest that coupling between the allosteric and active sites is mediated by a similarly positioned allosteric couple: Arg-187–Tyr-223 in caspase-7 and Arg-286–Glu-390 in caspase-1. Previous studies (23, 24) show that the conformational changes induced by binding of the allosteric compounds to either caspase-7 or caspase-1 are highly conserved despite them sharing only 23% sequence identity. One of the central challenges for generating selective and tight binding non-covalent active site inhibitors of the caspases is their common requirement for an acidic functionality in the P1-binding pocket, which have not to date produced drug-like compounds. The allosteric site in caspases offers an alternative because selective tethered compounds can be found for the executioner caspase-3/-7 or for inflammatory caspase-1. Our mutational and labeling experiments suggest that if one were to further optimize these allosteric inhibitors, it is worth focusing on optimization of the interaction between the compound and the L2' loop. Dissection of the allosteric mechanism is not only critical to our fundamental understanding of allostery but also facilitates our understanding of how to selectively inhibit caspases in cells. Finally, the allosteric transition from on (mature caspase-7) to off (in the presence of FICA or DICA) is imminently relevant to the zymogen form (procaspase-7), which is the predominant form of the enzyme in the absence of apoptotic stimuli. These studies broaden our understanding of how this transition occurs, and eventually, how specific small molecules may be used to reverse this transition in cells and even animals.

Acknowledgments—We thank all our former research colleagues at Sunesis Pharmaceuticals for support and encouragement in this work.

REFERENCES

- Fuentes-Prior, P., and Salvesen, G. S. (2004) *Biochem. J.* **384**, 201–232
- Yeretssian, G., Labbé, K., and Saleh, M. (2008) *Cytokine* **43**, 380–390
- Shi, Y. (2002) *Mol. Cell* **9**, 459–470
- Dix, M. M., Simon, G. M., and Cravatt, B. F. (2008) *Cell* **134**, 679–691
- Mahrus, S., Trinidad, J. C., Barkan, D. T., Sali, A., Burlingame, A. L., and Wells, J. A. (2008) *Cell* **134**, 866–876
- Lüthi, A. U., and Martin, S. J. (2007) *Cell Death Differ.* **14**, 641–650
- Reed, J. C., and Tomaselli, K. J. (2000) *Curr. Opin. Biotechnol.* **11**, 586–592
- Denault, J. B., and Salvesen, G. S. (2002) *Chem. Rev.* **102**, 4489–4500
- Howard, A. D., Kostura, M. J., Thornberry, N., Ding, G. J., Limjuco, G., Weidner, J., Salley, J. P., Hogquist, K. A., Chaplin, D. D., Mumford, R. A., et al. (1991) *J. Immunol.* **147**, 2964–2969
- Rotonda, J., Nicholson, D. W., Fazil, K. M., Gallant, M., Gareau, Y., Labelle, M., Peterson, E. P., Rasper, D. M., Ruel, R., Vaillancourt, J. P., Thornberry, N. A., and Becker, J. W. (1996) *Nat. Struct. Biol.* **3**, 619–625
- Thornberry, N. A., Rano, T. A., Peterson, E. P., Rasper, D. M., Timkey, T., Garcia-Calvo, M., Houtzager, V. M., Nordstrom, P. A., Roy, S., Vaillancourt, J. P., Chapman, K. T., and Nicholson, D. W. (1997) *J. Biol. Chem.* **272**, 17907–17911
- Garcia-Calvo, M., Peterson, E. P., Rasper, D. M., Vaillancourt, J. P., Zamboni, R., Nicholson, D. W., and Thornberry, N. A. (1999) *Cell Death Differ.* **6**, 362–369
- Chéreau, D., Kodandapani, L., Tomaselli, K. J., Spada, A. P., and Wu, J. C. (2003) *Biochemistry* **42**, 4151–4160
- Nuttall, M. E., Lee, D., McLaughlin, B., and Erhardt, J. A. (2001) *Drug Discov. Today* **6**, 85–91
- Chai, J., Wu, Q., Shiozaki, E., Srinivasula, S. M., Alnemri, E. S., and Shi, Y. (2001) *Cell* **107**, 399–407
- Riedl, S. J., Fuentes-Prior, P., Renatus, M., Kairies, N., Krapp, S., Huber, R., Salvesen, G. S., and Bode, W. (2001) *Proc. Natl. Acad. Sci. U.S.A.* **98**, 14790–14795
- Chai, J., Shiozaki, E., Srinivasula, S. M., Wu, Q., Datta, P., Alnemri, E. S., and Shi, Y. (2001) *Cell* **104**, 769–780
- Wei, Y., Fox, T., Chambers, S. P., Sintchak, J., Coll, J. T., Golec, J. M., Swenson, L., Wilson, K. P., and Charifson, P. S. (2000) *Chem. Biol.* **7**, 423–432
- Agniswamy, J., Fang, B., and Weber, I. T. (2007) *FEBS J.* **274**, 4752–4765
- Berger, A. B., Witte, M. D., Denault, J. B., Sadaghiani, A. M., Sexton, K. M., Salvesen, G. S., and Bogoy, M. (2006) *Mol. Cell* **23**, 509–521
- Denault, J. B., Békés, M., Scott, F. L., Sexton, K. M., Bogoy, M., and Salvesen, G. S. (2006) *Mol. Cell* **23**, 523–533
- Romanowski, M. J., Scheer, J. M., O'Brien, T., and McDowell, R. S. (2004) *Structure* **12**, 1361–1371
- Hardy, J. A., Lam, J., Nguyen, J. T., O'Brien, T., and Wells, J. A. (2004) *Proc. Natl. Acad. Sci. U.S.A.* **101**, 12461–12466
- Scheer, J. M., Romanowski, M. J., and Wells, J. A. (2006) *Proc. Natl. Acad. Sci. U.S.A.* **103**, 7595–7600
- Asbóth, B., Stokum, E., Khan, I. U., and Polgár, L. (1985) *Biochemistry* **24**, 606–609
- Hedstrom, L. (2002) *Chem. Rev.* **102**, 4501–4524
- Schechter, I., and Berger, A. (1968) *Biochem. Biophys. Res. Commun.* **32**, 898–902
- Datta, D., Scheer, J. M., Romanowski, M. J., and Wells, J. A. (2008) *J. Mol. Biol.* **381**, 1157–1167
- Gao, J., Sidhu, S. S., and Wells, J. A. (2009) *Proc. Natl. Acad. Sci. U.S.A.* **106**, 3071–3076
- Scheer, J. M., Wells, J. A., and Romanowski, M. J. (2005) *Protein Expr. Purif.* **41**, 148–153
- O'Brien, T., and Linton, S. D. (eds) (2009) *Design of Caspase Inhibitors as Potential Clinical Agents*, CRC Press, Inc., Boca Raton, FL